Predictions in Environmental Hydrodynamics Using the Finite Element Method II. Applications

S. W. ZELAZNY* AND A. J. BAKER†
Bell Aerospace Division of Textron, Buffalo, N.Y.

Two distinctly different problem classes in three-dimensional environmental hydrodynamics are solved using the computational embodiment of the finite element solution algorithm described in Part I. Pollutant dispersion in a river is studied as a function of turbulence modeling by solution of the governing parabolic equation system. The meandering flow of a natural river is analyzed through solution of an integral transformation of the full Navier-Stokes equations. Emphasis is placed on demonstrating the usefulness and versatility of the computational procedure for assessing and evaluating the controlling factors of specific environmental problems.

Introduction

A FINITE element numerical solution algorithm for complex flow problems characterized by either three-dimensional boundary region or integral-transform Navier-Stokes equations was presented in Part I.[1] Studies on accuracy, convergence, and over-all performance of the solution algorithm have been reported.[2,3] Herein, this analysis capability is exercised to demonstrate versatility for studying the physical phenomena which are often the controlling factors in characterizing environmental flow problems. In the first part of this paper the importance of accurately characterizing turbulent diffusion processes is assessed and the sensitivity of predictions to the turbulence model is determined for unidirectional flowfield. This section is followed by an analysis of flowfields containing high curvatures and recirculation zones, including a meandering river and a stream with an imbedded solid obstacle.

Numerical Results

Examination of the governing equation sets[1] shows that their closure requires specification of the effective viscosity, Prandtl number, and Lewis number. For laminar flows, these parameters are known explicitly in terms of local flow composition and temperature; however, for turbulent flow, empirical relations are required to characterize the mass, momentum, and energy diffusion. The approaches taken in predicting turbulence diffusion can be classified into two categories. The most commonly used method involves direct specification of an eddy viscosity model using empirical correlations. The second category includes any method wherein at least one additional equation is introduced, for example, the turbulence kinetic energy equation. Examples of turbulence flow problems solved using this latter technique are reported in Refs. 4–7. For the purposes of the sample computations reported herein, the empirical eddy kinematic viscosity models reported by Fisher[8,9] were used. Note, however that the computational procedure[1] is readily adaptable to considering higher order turbulence models.

Following Refs. 9 and 10, for the pollutant dispersion study involving the boundary region Navier-Stokes system, the Prandtl and Lewis numbers, hence Schmidt number, are assumed equal to unity. The eddy kinematic viscosity in the vertical and transverse (x_3, x_2) directions are assumed given by the forms

$$\varepsilon_{13} = k_3 U^* h \tag{1}$$

$$\varepsilon_{12} = k_2 U^* h \tag{2}$$

where the friction velocity $U^* = (\tau/\rho)^{1/2}$, and τ is calculated from[11]

$$\tau = K^2 \rho \tilde{U}^2 (R_*^{-1} - 0.156 R_*^{0.45} + 0.08723 R_*^{0.3} + 0.0371 R_*^{-0.18}) \tag{3}$$

here K is an empirical constant equal to 0.435, $R_* = K^2 R$ and $R = \tilde{U} x_3/\nu$. The length scale $\tilde{x}_3$ represents the thickness of the narrow region just above the waterway floor where convective flow effects are negligible, i.e., the constant shear stress region. Similarly $\tilde{U}$ represents the streamwise velocity component at the edge of the constant shear stress region whereas ν represents the laminar kinematic viscosity. Values for $\tilde{U}$ and $\tilde{x}_3$ are obtained directly from the solution if details of the velocity profile are being computed (as in this case). Values for $\tilde{U}$ and $\tilde{x}_3$ may also be obtained by assuming that the streamwise velocity may be expressed by a similarity profile, e.g., for turbulent flows a logarithmic velocity distribution would be employed.

Three predictions were made to determine dispersion sensitivity to the selected form of the eddy diffusion coefficients. These cases correspond to the following constants appearing in Eqs. (1) and (2).

$$\text{Case I: } k_2 = 0.23 \qquad k_3 = 0.067 \tag{4}$$

$$\text{Case II: } k_2 = 0.23 \qquad k_3 = 0.36(\xi - \xi^2) \tag{5}$$

$$\text{Case III: } k_2 = k_3 = (0.23^2 + 0.067^2)^{1/2} = 0.24 \tag{6}$$

In Eq. (5), $\xi = (x_3 - x_3^0)/h$ and x_3^0 is the river bottom coordinate. Although experimental results confirm that the vertical

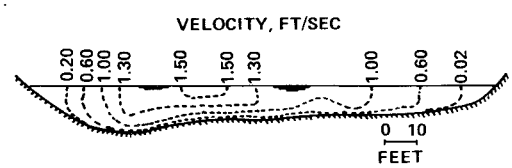

Fig. 1 A typical cross-section of a natural stream, showing isovels, after Ref. 8.

Presented as part of Paper 74-7 at the AIAA 12th Aerospace Sciences Meeting, Washington, D.C., January 30–February 1, 1974; submitted May 31, 1974, revision received August 12, 1974. The authors are grateful to J. Orzechowski who programed COMOC and performed many of the calculations reported herein and P. Manhardt who assisted in many ways.

Index categories: Hydrodynamics; Viscous Nonboundary-Layer Flows.

* Research Scientist, Computational Continuum Mechanics. Member AIAA.

† Principal Scientist, Computational Continuum Mechanics. Associate Fellow AIAA.

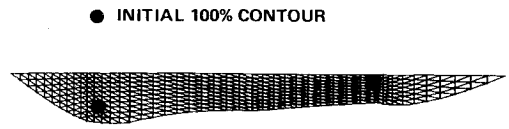

Fig. 2 Finite element discretization of cross-section of a natural stream.

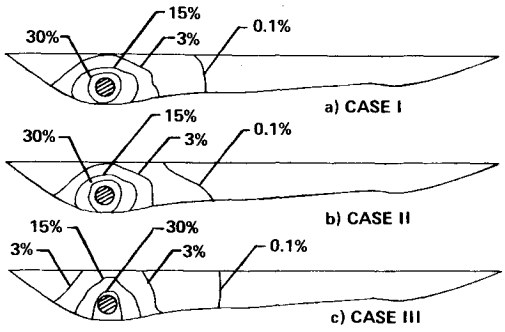

Fig. 3 Predicted mass fraction contours of 32.0 ft downstream of injection for three different types of diffusion coefficients.

mixing coefficient exhibits a parabolic distribution across the river depth, the use of depth mean averages has been suggested.[8] Cases I and II evaluate the consequence of neglecting the parabolic distribution; the constants for these cases were taken from Ref. 8. Case III examines the importance of tensorial ($\varepsilon_{12} \neq \varepsilon_{13}$) rather than scalar diffusion coefficients. The selected cross-section depth distribution and measured velocity contours in an actual river[8] are shown in Fig. 1. The finite element discretization, employing 468 elements is shown in Fig. 2, as well as the initial concentration field, i.e., regions with and without contaminant, at the start of computation. Predicted concentration contours are shown in Fig. 3 for Cases I–III at 9.6 m downstream of injection of the contaminant. Comparing the concentration contours of Figs. 3a and 3b shows that neglect of the parabolic distribution in the vertical mixing coefficient is a reasonable assumption for these selected conditions. On the other hand, the effect of a tensorial diffusion coefficient was found to be quite measurable as seen by comparing Figs. 3a and 3c. Figure 4 shows a plan view (x_1, x_2 plane) of the pollutant dispersion pattern for the 3% contour line for the three cases. Note that the dispersion pattern in the plan view is consistent with observations in the x_2, x_3 plane;

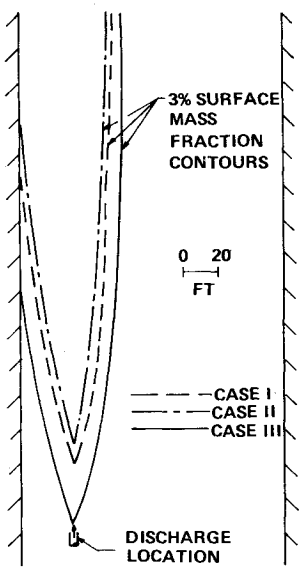

Fig. 4 Top view of natural stream showing contours along which the concentration of effluent has reached 3% at the surface.

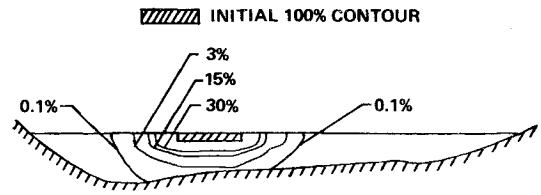

Fig. 5 Predicted mass fraction contours at 32.0 ft downstream of interface injection, Case IV.

i.e., neglecting the tensorial nature of the diffusion coefficient has a significant effect on the rate at which the effluent is diffused to the surface (the 3% contour of Case III reaches the surface 8.5 m before the 3% contour of Case I).

An additional case was considered to study the effect of the initial location and profile of the contaminant on diffusion. As shown in Fig. 5, the initial contour for Case IV assumes injection of a contaminant on the water surface. The predicted concentration distributions, Fig. 5, show that mixing was slightly greater in the deeper part of the river, in agreement with the concept that the diffusion coefficients are directly proportional to local depth. In comparing Cases I and IV, for the identical turbulence model, the initial shape and location had only minor effect on the over-all mixing. For example, for Case I, the 3% contour line penetrated the uncontaminated region of the river a maximum distance of 8 m as compared to 4 m for Case IV. This may primarily reflect the basic simplicity of the turbulence model. Experience in modeling turbulence in boundary layers[12] and free shear flows[13] has clearly shown that simple eddy viscosity relations such as Eqs. (1) and (2) are applicable only to the narrow range of flow conditions for which the constants were determined. In addition, the recent success of some higher order turbulence models in accurately predicting diverse types of flow conditions,[4–7] suggests these methods be considered for predicting environmental flowfields of the type discussed.

A basic character of flow in natural waterways is the tendency to meander, as amply illustrated by recent ERTS photographs of large river systems. An initially straight-flowing river is in neutral stability in the sense that minor nonuniformities in the flow will eventually cause preferential bank and river bed erosion resulting in the typical meander geometry. The mechanisms of water transport in a meandering river preferentially erode the far bank of a bend which in turn tends to make the meander grow. Alteration of the river bed via erosion and deposition of silt are a complicated consequence of this action. A complex combination of inertial, centrifugal, and viscous forces combine to produce this phenomenon about which little detailed information is known other than the experimental determination of dispersion coefficients.[9] Numerical solution of the integral Navier-Stokes formulation can provide insight into the controlling mechanisms of the phenomenon; the generality of the finite element approach allows inclusion of the all-important geometry factors of nonuniform depth, nonregular channel shape, hence capture of the physical essence of the problem is possible.

Shown in Fig. 6 is an illustration of a typical meander geometry[9] assumed as an outlet from a large reservoir. Shown in Fig. 7 is a finite element discretization of the same geometry,

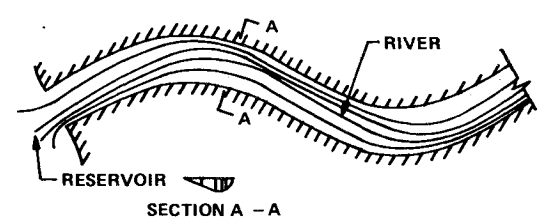

Fig. 6 Illustration of typical meander geometry, after Ref. 9.

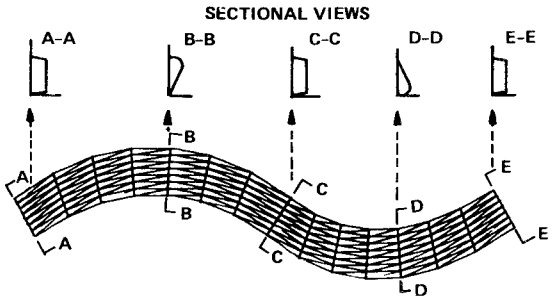

Fig. 7 Finite element discretization of meandering river and sectional views of varying riverbed depth.

employing 196 elements, as well as the variation in channel cross-sectional depth distribution used for numerical experimentation purposes. The length span of the river is approximately 73 m (240 ft), the cross-sectional median width is 6 m (18 ft), and the mean depth 1.83 m (6 ft). A flow Reynolds number is 0.17×10^7 based upon channel width and uniform inlet velocity of 0.31 m/sec (1 fps). For these predictions, the turbulent transport coefficient was assumed a scalar equal in magnitude to a representative average (0.1 m^2/sec) of experimentally measured transverse mixing coefficients in natural meandering flows.[9] Both river banks were assumed no-slip walls for vorticity and a vanishing normal gradient for all dependent variables was applied at the downstream outflow location. Illustrated in Fig. 8 are the computed steady-flow, equal-discharge streamtube distributions for inlet velocities of 0.31 m/sec and 1.84 m/sec as well as the streamtube distribution for potential (inviscid) flow. The predicted parallel streamline distribution for potential flow, Fig. 8a, indicates adequate solution accuracy for the selected finite element discretization of the solution domain. Close examination of the Fig. 8b shows a modest flow concentration at the inside of each bend; the retarding influence of the river banks is also evident. The latter case (Fig. 8c) predicts flow separation at the outside of the second bend and formation of a dead water region. No special techniques are required to encourage prediction of recirculation regions, as commonly occurs for finite difference procedures.[14-17] Other results have illustrated the accuracy of similar predictions for recirculating flows that are experimentally verifiable.[2] Shown in Figs. 9 and 10 are computed steady-flow streamwise velocity distributions across each river bend, and at the midpoint between bends, in comparison to the (assumed) uniform inlet profile. The predicted skewness in the

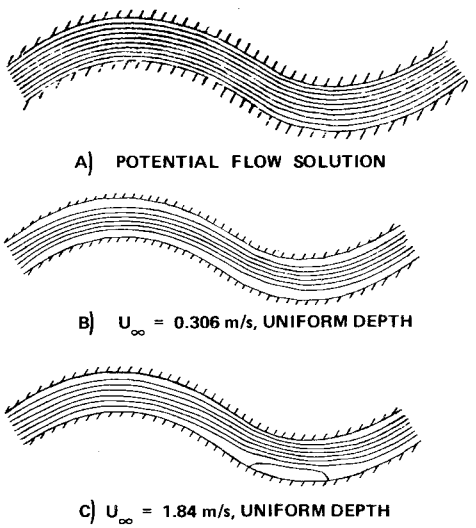

Fig. 8 Equal discharge streamtube distribution for meandering flows.

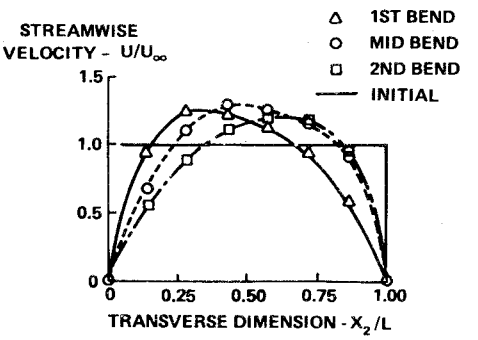

Fig. 9 Streamwise velocity distribution in uniform depth meandering river, Re = 0.17E7.

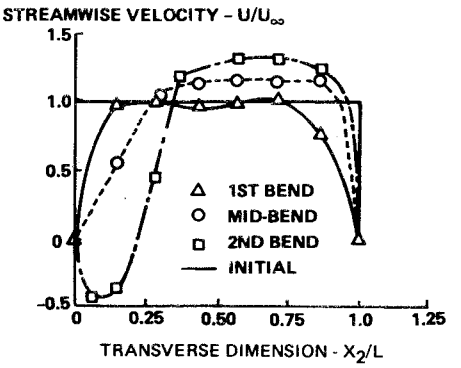

Fig. 10 Streamwise velocity distribution in uniform depth meandering river, Re = 0.1E8.

distributions of Fig. 9 illustrates the influence of curvature of the river banks; the predicted dead water region yields the negative velocities in Fig. 10. Figure 11 illustrates the computed river bank shear stress distribution.

An analysis of crucial impact for predictions in environmental hydrodynamics is accurate prediction of flows containing imbedded regions of recirculation. Wharfs, piers, break-walls, jetties, as well as naturally occurring obstructions, all produce this phenomenon. Each of these can significantly alter the attendant shear-stress distribution on surrounding flow boundaries which can lead to adverse erosion phenomena. A basic understanding of the influence on the environment, of man's design for such structures, can come from numerical computation of genuine simulations of the flow geometry. A basic study problem that assesses the accuracy of recirculation predictions is flow in a confined channel with a sudden increase in cross-sectional

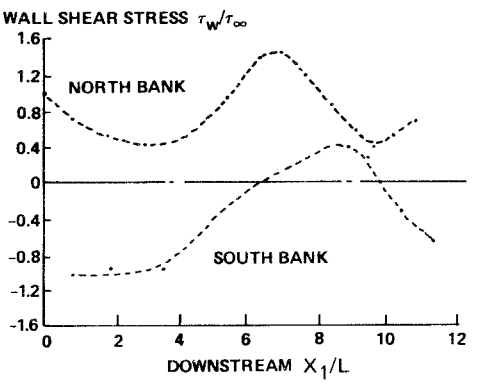

Fig. 11 Wall shear stress distributions for meandering flow, Re = 0.1E(8).

Fig. 12a Computed steady-state streamfunction and vorticity for flow over a rearward step, $Re = 200$.

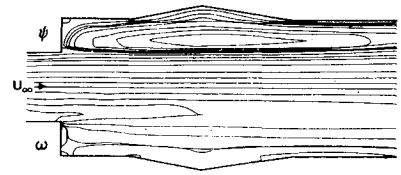

Fig. 12b Computed steady-state streamfunction and vorticity for flow over a rearward step in irregular shaped duct, $Re = 200$.

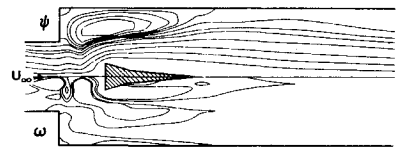

Fig. 12c Computed steady-state streamfunction and vorticity for flow over a rearward step with internal obstacle, $Re = 200$.

area. This "rearward facing step" geometry is experimentally verified to produce a steady-state recirculation region downstream of the step with attachment points located at the step and downstream wall as a function of Reynolds number.[15,18] Accurate prediction of the extent of the recirculation zone without resort to any special boundary condition constraints is discussed in Ref. 2. Shown in Fig. 12 are closeups of the predicted recirculation region for the parent problem and variations involving an indented wall and an internal obstacle. The latter geometry drastically alters the location and strength of the recirculation zone, and the attendant change in wall shear stress distribution is shown in Fig. 13. Designs of this type introduced into environmental flows could certainly have an adverse affect on river bank erosion. These results amply illustrate how the numerical solution procedure could be utilized as an engineering design tool to optimize flow confinement construction while minimizing adverse ecological effects.

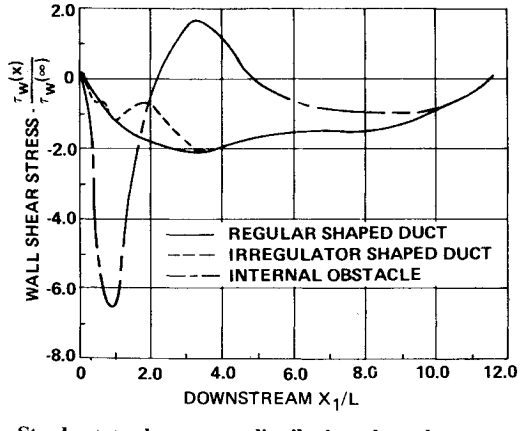

Fig. 13 Steady-state shear stress distribution along downstream wall for flow over a rearward step.

Conclusions

A computer program embodying a finite element solution algorithm has been developed for two equation systems covering a wide range of practical three-dimensional flow problems in environmental hydrodynamics. Sample computations of waste water discharge and meandering rivers with recirculation zones were presented. Variations on empirical relations for the eddy transport coefficients were studied. Results suggest that higher order turbulence models are required to accurately characterize turbulent diffusion phenomena for diverse types of flow conditions. The computational procedure appears highly useful for complementing analysis and experimental design studies for evaluation of ecological impact of proposed hydrodynamical flow systems.

References

[1] Baker, A. J., "Predictions in Environmental Hydrodynamics Using the Finite Element Method—Part I: Theory," *AIAA Journal*, Vol. 13, No. 1, Jan. 1975.

[2] Baker, A. J., "A Finite Element Solution Algorithm for the Navier-Stokes Equations," CR-2391, 1974, NASA.

[3] Baker, A. J. and Zelazny, S. W., "A Theoretical Study of Mixing Downstream of Transverse Injection into a Supersonic Boundary Layer," CR-112254, 1972, NASA.

[4] Launder, B. E. and Spalding, D. B., *Mathematical Models in Turbulence*, Academic Press, London and New York, 1972.

[5] Donaldson, C. duP and Sullivan, R. D., "An Invariant Second Order Closure Model of the Compressible Turbulent Boundary Layer on a Flat Plate," CR-128172, June 1972, NASA.

[6] Lilley, D. G., "Prediction of Inert Turbulent Swirl Flows," *AIAA Journal*, Vol. II, No. 7, July 1973, pp. 955–960.

[7] Rhodes, R. P., Harsha, P. T., and Peters, C. E., "Turbulent Kinetic Energy Analysis of Hydrogen-Air Diffusion Flames," presented at the 4th International Colloquim on Gas Dynamics and Explosions and Reactive Systems, July 1973.

[8] Fischer, H. B., "Longitudinal Dispersion and Turbulent Mixing in Open Channel Flow," *Annual Review of Fluid Mechanics*, Vol. 5, May 1973, pp. 59–78.

[9] Fischer, H. B., "The Effect of Bends on Dispersion in Streams," Water Resources Research, Vol. 5, No. 2, May 1969, pp. 496–506.

[10] Jobson, H. E. and Sayre, W. W., "Vertical Transfer in Open Channel Flow," *Proceedings of the American Society of Chemical Engineers, Journal of Hydronautics Division*, Vol. 96, 1970, 703–724.

[11] Patankar, S. V. and Spalding, D. B., *Heat and Mass Transfer in Boundary Layers*, Intertext Books, London, England, 1970, p. 72.

[12] Kline, S. J., Morkovin, M. V., Sovran, G., and Cockrell, D. J., eds., *Proceedings, Computation of Turbulent Boundary Layers*, Stanford University, Stanford, Calif., 1968.

[13] *Proceedings of the NASA Workshop on Free Turbulent Shear Flows*, Vol. I, SP-321, July 1972, NASA.

[14] Gosman, A. D., Pun, W. M., Runchal, A. K., Spalding, D. B., and Wolfshtein, M., *Heat and Mass Transfer in Recirculating Flows*, Academic Press, London, 1969.

[15] Mueller, T. J. and O'Leary, R. A., "Physical and Numerical Experiments in Laminar Incompressible Separating and Reattaching Flows," AIAA Paper 70-763, Los Angeles, Calif., 1970.

[16] Macagno, E. O. and Hung, T. K., "Computational and Experimental Study of a Captive Annular Eddy," *Journal of Fluid Mechanics*, Vol. 28, No. 1, Jan. 1967, pp. 43–64.

[17] Roache, P. J. and Mueller, T. J., "Numerical Solutions of Laminar Separated Flows," *AIAA Journal*, Vol. 8, No. 3, March 1970, pp. 530–538.

[18] Dorodnitsyn, A. A., "Review of Methods for Solving the Navier-Stokes Equations," *Proceedings of the Third International Conference on Numerical Methods in Fluid Mechanics*, 1973, pp. 1–11.